© 2014. Published by The Company of Biologists Ltd | The Journal of Experimental Biology (2014) 217, 2445-2448 doi:10.1242/jeb.097634

SHORT COMMUNICATION

Highly extensible skeletal muscle in snakes

Matthew Close[1,2,*], Stefano Perni[3,4], Clara Franzini-Armstrong[3] and David Cundall[1]

ABSTRACT

Many snakes swallow large prey whole, and this process requires large displacements of the unfused tips of the mandibles and passive stretching of the soft tissues connecting them. Under these conditions, the intermandibular muscles are highly stretched but subsequently recover normal function. In the highly stretched condition we observed in snakes, sarcomere length (SL) increased 210% its resting value (SL_0), and actin and myosin filaments no longer overlapped. Myofibrils fell out of register and triad alignment was disrupted. Following passive recovery, SLs returned to 82% SL_0, creating a region of double-overlapping actin filaments. Recovery required recoil of intracellular titin filaments, elastic cytoskeletal components for realigning myofibrils, and muscle activation. Stretch of whole muscles exceeded that of sarcomeres as a result of extension of folded terminal tendon fibrils, stretching of extracellular elastin and independent slippage of muscle fibers. Snake intermandibular muscles thus provide a unique model of how basic components of vertebrate skeletal muscle can be modified to permit extreme extensibility.

KEY WORDS: Comparative myology, Gape, Intermandibular soft tissues, Macrostomy, Passive extensibility, Titin

INTRODUCTION

Skeletal muscles have passive elastic properties resulting from a combination of components: titin filaments within the sarcomeres, an internal cytoskeletal network, an extensible sarcolemma (membrane plus basal lamina), and collagen and elastin fibers in extracellular connective tissues (Wang et al., 1993). The sarcolemma and extracellular connective tissues determine how far a muscle can stretch without breaking (Dulhunty and Franzini-Armstrong, 1975). Extension of skeletal muscles *in vivo* is usually limited to lengths that lie within the range of overlap of actin and myosin filaments. However, a striking exception is a bilaterally paired, transversely oriented muscle connecting the unfused mandibular tips of colubroid snakes – the m. intermandibularis anterior, pars anterior (MIAA). During swallowing, the distance between the right and left mandibular tips increases greatly, presumably imposing high levels of strain on the MIAA. The functions of this muscle and other closely associated intermandibular soft tissues (Close and Cundall, 2014) serve as major determinants of gape in snakes. The degree to which the MIAA extends during feeding events is currently undefined for any snake, and the problem of recovery from levels of extension that could be beyond the physiological limits of contraction have yet to be investigated.

We sought to determine what features (1) limit MIAA extension and (2) provide a structural basis for recovery from extremely high levels of extension. We first recorded the behavior of the lower jaw during swallowing events to define normal limits to extensibility. We then determined the anatomical and histological effects of extension and recovery by experimentally manipulating lower jaws excised from freshly killed snakes to levels of extension observed during swallowing. Finally, we determined the consequences of stretch and recovery at the cellular level by comparing the ultrastructure of resting, stretched and recovered fibers.

RESULTS AND DISCUSSION

Analysis of laboratory video records of northern watersnakes, *Nerodia sipedon* (Linneaus 1758), swallowing fishes showed that the maximum distance reached between the tips of the mandibles (intermandibular distance) was 770% of resting intermandibular distance (Fig. 1A,B) and required up to 20 min to attain. Intermandibular distance was positively correlated (r^2=0.35) with ingestion ratio, the ratio of the cross-sectional area of the prey to the cross-sectional area of the snake's gape, showing that ingestion of larger prey requires greater extension of the intermandibular soft tissues (e.g. muscle; Fig. 1C,D). The total 770% increase in intermandibular distance experienced can thus be seen as the sum of increases in left and right slips of the MIAA and their midline insertion (interramal pad; Fig. 1C,D).

We compared the anatomy and ultrastructure of the MIAA in resting, stretched and recovered lower jaws from size-matched adult watersnakes. Lengths of stretched muscles were 270% those of resting specimens, but average sarcomere length (SL) for stretched muscle fibres was only ~210% of resting length (SL_0) (supplementary material Table S1). In contrast to myofilament arrangement in resting fibers (Fig. 2A), actin and myosin filaments in stretched fibers failed to overlap, creating a gap region (supplementary material Table S1; Fig. 2B) spanned presumably by superthin (titin) filaments (Salviati et al., 1990). Average Z-line to A-band distance was 1.9±0.33 µm, and was within the range of titin extension (Salviati et al., 1990). Cross-striations were misaligned, significantly increasing distances between Z-lines of adjacent myofibrils in the longitudinal direction in stretched fibers (P<0.01; supplementary material Table S1; Fig. 2F,G). Stretching also resulted in distortion of the sarcoplasmic reticulum including the position of some triads (Fig. 2I,J).

In recovered fibers, the gap region disappeared and myofilament overlap was re-established (Fig. 2C). However, average SL was significantly shorter than in resting fibers (P<0.01; supplementary material Table S1), and actin filaments from adjacent hemisarcomeres overlapped in the middle of the sarcomere (Fig. 2C,D). There were no apparent damaged ('popped') sarcomeres as seen in skeletal muscle that has been stimulated at high levels of extension. Alignment of both Z-lines (Fig. 2H) and triads (Fig. 2K) was restored in recovered fibers, supporting the

[1]Department of Biological Sciences, 1 W. Packer Avenue, Lehigh University, Bethlehem, PA 18015, USA. [2]Biology Department, Radford University, Box 6931, Radford, VA 24142, USA. [3]Department of Cell and Developmental Biology, University of Pennsylvania, Philadelphia, PA 19104-6058, USA. [4]Department of Physiology and Biophysics, University of Colorado Anschutz Medical Campus, Aurora, CO 80045, USA.

*Author for correspondence (mclose2@radford.edu)

Received 27 September 2013; Accepted 17 April 2014

The Journal of Experimental Biology (2014) doi:10.1242/jeb.097634

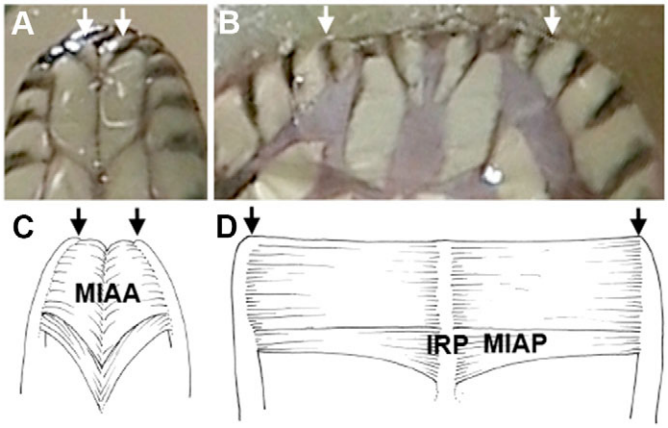

Fig. 1. Gross anatomical effects of lateral lower jaw extension during swallowing. (A,B) Video fields taken from a recording of an adult watersnake (*Nerodia sipedon*) ingesting a trout. (A) Resting; white arrows indicate the approximate locations of the mandibular tips. (B) Stretched; white arrows as in A. The stretched intermandibular distance is ~650% resting distance. (C,D) Illustrations showing the relationships of intermandibular muscles to the mandibles (origin) and interramal pad (midline insertion) in the resting (C) and stretched (D) conditions. Black arrows indicate the locations of the mandibular tips. The stretched intermandibular distance is ~600% resting distance. IRP, interramal pad; MIAA, m. intermandibularis anterior, pars anterior; MIAP, m. intermandibularis anterior, pars posterior.

existence of elastic elements in both myofibrillar and cytoskeletal architecture.

At a minimum, two components must be involved in length recovery. Initial shortening depends on passive elastic properties, as there is no myofilament overlap to facilitate contraction (Fig. 2B,E). Models of titin's function, generated primarily from studies of the isolated protein, show it can extend reversibly to lengths of 1.5–4 μm (Linke et al., 1998). However, there has been little evidence of titin's ability to passively restore muscle from high levels of extension *in vivo* under normal physiological conditions in vertebrates. The MIAA of snakes serves as a test of this function *in vivo* because the muscle is regularly stretched beyond myofilament overlap when snakes swallow large prey. It does not, however, explain the recovery of myofibrillar and membrane arrangements. This might be due to a second set of elastic cytoskeletal proteins between myofibrils (Wang and Ramirez-Mitchell, 1983) and by default membrane realignment occurring as myofibrils realign themselves.

The second event results in the double overlap of actin filaments from adjacent hemisarcomeres (Fig. 2C,D), a state previously seen in contracted muscle exclusively. The final sarcomere length following removal of load after extreme strain may involve muscle activation, or it could be a function of the molecular and mechanical events associated with the recoil/refolding of titin from its extended state during extremely high strains (Tskhovrebva et al., 1997). As the recovery achieved in the MIAA occurred in the absence of direct stimulation, it is possible that if contraction did occur, full recovery was achieved by mechanically induced activation resulting from neurotransmitter release from motor end plates, ion fluxes around disrupted triads, or tears in the sarcoplasmic reticulum resulting from strains imposed during stretching.

The relative increase in SL in the highly stretched muscle is less than that of the whole muscle (supplementary material Table S1). A similar occurrence was reported previously in the tongue retractor muscle of an agamid lizard (*Pogona vitticeps*), in which SL

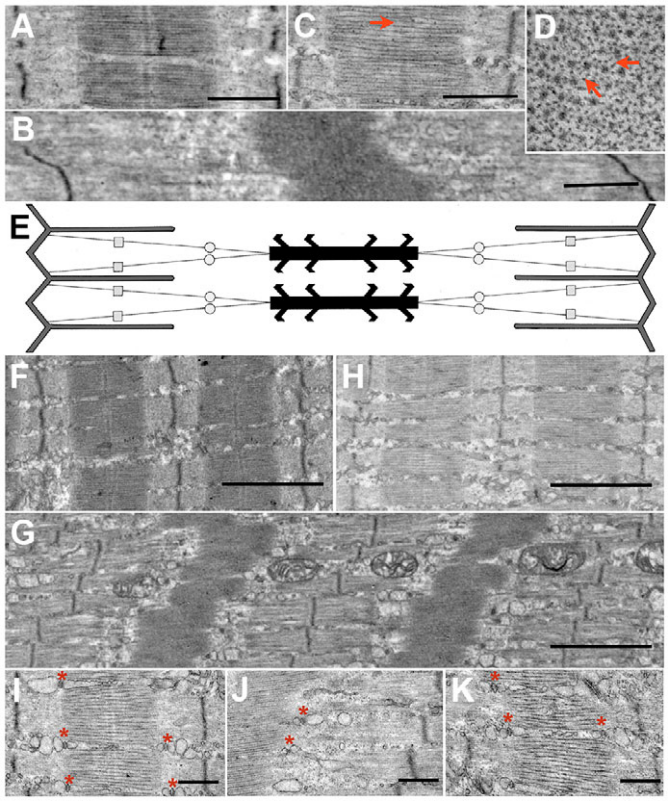

Fig. 2. TEM micrographs of resting, stretched and recovered watersnake intermandibular muscles. (A–C) Longitudinal sections of sarcomeres in the resting (A), stretched (B) and recovered (C) condition. Arrows indicate areas of double-overlapping actin filaments in the middle of sarcomeres. Scale bars, 0.5 μm. (D) Cross-section of part of a recovered myofibril at 96,800× magnification showing double-overlap of thin filaments at mid-sarcomere. (E) Two-dimensional model of a highly stretched sarcomere incorporating the current model for unactivated titin. Squares represent the N2A region and circles represent -the border of the PVEK and distal tandem immunoglobulin (Ig) segments of the titin molecule. For simplicity, only two of the six titins for each hemisarcomere are shown. Titin may provide positional stability of myofilaments at high degrees of stretch: refolding/recoiling of the molecule is postulated to guide thin filaments back into position. However, double overlap seen in recovered muscle requires active contraction. (F–H) Longitudinal sections of fibers at lower magnification showing the Z-line relationship between adjacent myofibrils in resting (F), stretched (G) and recovered (H) fibers. Scale bars, 2.0 μm. The Z-lines become staggered or misaligned as a result of stretching (G), but recover after loads are released (H). (I–K) Longitudinal sections of resting (I), stretched (J) and recovered (K) fibers showing alignment of triads (*) with the end of the A-band. In the stretched condition, the triads remain close to the A-band but their alignment is not uniform and there is some distortion of the terminal and intermediate cisternae (J), both of which regained normal morphology (I) upon recovery (K). Scale bars, 0.5 μm.

increased by only 120% for a total muscle extension of 150% (Herrel et al., 2002). This discrepancy arises from a third component of stretching involving adaptation of connective tissues surrounding muscle fibers (Purslow, 1989). Comparisons of cross-sections of resting and stretched whole muscles reveal that fibers that are normally polygonal in shape and compactly arranged in the resting condition take on cylindrical cross-sectional shapes and are spaced farther apart when stretched (supplementary material Fig. S1a,b). Changes in the cross-sectional area of cells require adjustments of the surrounding extracellular matrix (ECM) to these mechanical events. Studies of the perimysium have shown that collagen fibers

The Journal of Experimental Biology

will reorient themselves in response to extension (Purslow, 1989), and that rate-dependent, non-linear viscoelastic behaviors of collagen (stress–relaxation and creep) are possibly rooted in the properties of the fibers themselves or in the interactions of the fibers with the surrounding matrix (Purslow et al., 1998). Numerous records of snakes feeding indicate that swallowing large prey is a process occurring slowly over a long period of time. The relatively low strain rates would therefore provide ideal conditions for non-linear viscoelastic responses of both cells and surrounding tissues to occur.

The histological organization of muscle fibers might underlie some of the tensile properties of whole muscle and its ability to resist damage resulting from exceedingly high tensile strain. Our light micrographs of the stretched condition show that the ends of MIAA muscle fibers do not line up at their site of attachment, suggesting a difference in the lengths of tendon fibrils between adjacent fibers (supplementary material Fig. S1c). This permits whole muscle to extend beyond the limits of extension of its individual fibers by permitting slippage of adjacent fibers during extension. A second role of the ECM then involves returning whole muscle to its resting state via passive elastic recoil – a role fulfilled by elastin in the ECM. Our light micrographs show that elastin is distributed throughout the MIAA, at myotendon junctions and within both perimysia and epimysia (supplementary material Fig. S1c–e). This combination of variable tendon fibril lengths and widespread distribution of elastin provides a mechanism to permit a great deal of slippage of adjacent fibers and passive return of whole muscle to its resting configuration following an extremely high level of extension (supplementary material Fig. S1f).

Our ultrastructural and histological results indicate that hyperstretched myofibrils are passively restored to their resting state by recoil of superthin intracellular filaments (Fig. 2E), while a network of extracellular elastin contributes to restoring muscle fibers to their resting position within the whole muscle (supplementary material Fig. S1f). During swallowing, the degree of extension and the amount of time involved may be greater than in the specimens we prepared for ultrastructural study. Unless sarcomeres stretch further, this would increase the discrepancy between overall muscle length and SL. SL upon immediate recovery is 18% shorter than SL_0, whereas muscle length is within 4% of initial length, suggesting that fiber and sarcomere recovery processes differ from whole-muscle recovery. The former is explained primarily by elastic recoil of stretched intracellular titin (Tskhovrebova et al., 1997) while the latter involves properties within and between collagen fibers (Purslow, 1989; Purslow et al., 1998) and elastic recoil of elastin fibers in the ECM.

Macrostomy is a feature of many snake taxa. Although the skeletal modifications that allowed for increased gape in snakes are well known, soft tissue properties are not. Our results show that the intermandibular muscles of snakes attain levels of extensibility that surpass the physiological limits of most vertebrate skeletal muscles, accomplished by modifications at cellular and subcellular levels. Snakes thus provide a unique model for testing hypotheses of soft tissue behaviors and the role that soft tissues play in the evolution of extreme functions.

MATERIALS AND METHODS

Feeding events (164 in total) were recorded with a Panasonic AG-456 camcorder for 10 adult and 15 juvenile and neonate *N. sipedon*. Snakes were fed fish (*Notemigomus crysoleucas*, *Oncorhynchus mykiss*, *Pimephales promelas*, *Salmo trutta* and *Salvelinus fontinalis*) of masses scaled to premeasured intervals of snake mass, ranging from 20 to 90%. Fish maximum height and width was measured prior to feeding. These measures were later used to generate estimates of prey cross-sectional area, and these were combined with estimates of snake gape cross-sectional area to provide an ingestion ratio (prey cross-sectional area/snake gape). A subset of 49 feeding records for which the mass ratio was greater than 30% were then used to determine the limits to lower jaw extensibility. Video records included ventral views of the lower jaw showing the tips of the mandibles (intermandibular distance) at rest and at maximum gape during swallowing and also provided a time base for events. Intermandibular distance measured solely from the ventral view does not take into account displacement imposed on the lower jaw soft tissues in the direction of the camera by prey, and may thus underestimate stretching. Given that the prey species used in our study were fish with relatively large body height to width ratios that were always oriented sideways when ingested, the effects imposed were likely minimal. We then used univariate general linear regression of ingestion ratio (x) on change in intermandibular distance (y) to determine the relationship between increasing relative prey size and change in intermandibular distance. Our behavioral records established the normal timing and limits of strain of the intermandibular soft tissues, values we replicated during manual manipulations (Close and Cundall, 2014).

Ultrastructural analysis was based on muscles from three adult northern watersnakes of approximately the same size (average jaw length 28.3±2.0 mm). Adults were used because the relatively small size of neonates and juveniles made it difficult to skin and manipulate the lower jaw and subsequently measure and fix muscle tissues within these size classes in a timely manner. Snakes were killed via decapitation following anesthesia, and lower jaws of snakes were removed and skinned in an isotonic snake Ringer's solution. Exposed MIAA muscles were kept wet with this solution during all experimental manipulations. Specimens were divided into three categories: resting, stretched and recovered. The lower jaw of the resting specimen received no treatment. To stretch lower jaws of the stretched and recovered specimens, we first pinned the right mandible of each specimen to a dissecting tray and then sutured the left mandible to a wooden dowel held by a micromanipulator. Using the micromanipulator, we stretched the lower jaw of both specimens a rate of 2 mm every 5 min (17% resting length per minute) until the desired degree of intermandibular extension was obtained (~700% resting intermandibular distance). The stretched specimen was fixed at peak extension, but the mandible of the recovered specimen was detached from the micromanipulator and, prior to fixing, the lower jaw was allowed to recover while examined with a dissecting microscope until shortening was no longer detectable. Intermandibular distance and approximate muscle length for right and left MIAA muscles were measured prior to the stretch period, at peak extension and following fixation using a miniscale or dial calipers. Following treatment, all specimens were fixed in an 8% 0.1 mol l^{-1} sodium cacodylate-buffered glutaraldehyde solution for 45 min prior to extraction of the muscles from the lower jaw. Finally, muscles were removed and stored in 4% glutaraldehyde.

For EM imaging, the tissue was post-fixed in buffered 2% OsO_4 for 1 h at 4°C, en bloc stained with uranyl acetate and embedded in Epon. Thin sections were stained with lead citrate after cutting and examined in a Philips 410 electron microscope (Philips Electron Optics, Mahwah, NJ, USA). The images were recorded digitally with a Hamamatsu C4742-95 digital camera (Advanced Microscopy Techniques, Chazy, NY, USA). We measured intra-sarcomere distances using Fiji software, and interfibrillar Z-line distances were measured using ImageJ software (US National Institutes of Health, Bethesda, MD, USA). Means were compared using Student's t-tests in Microsoft Excel 2010.

In order to determine the effects of stretching on whole muscle, thick cross-sections from Epon-embedded resting and stretched samples from random points along the middle and ends of the muscle were cut and stained with Toluidine Blue. Because serial sections were not taken, it was impossible to determine how many fibers might be tapered. Images were then projected on a screen and muscle fibers were outlined, traced and shaded in order to improve contrast and reveal fiber shape/cross-sectional area of each condition. Finally, a paraffin-embedded, moderately stretched watersnake lower jaw was sectioned in transverse and longitudinal planes.

To determine the occurrence and distribution of collagen and elastin in the endomysia, perimysia and epimysia of the MIAA, sections were subsequently stained with H&E and iron gallein elastin stain, mounted and viewed using compound light microscopy. Because both transverse and longitudinal sections were made from the same specimen, and because serial sections were not used, it was impossible to trace individual fibers. However, because multiple regions were sampled (i.e. muscle belly and insertion), the histological material provided an estimate of elastin distribution.

All methods were approved under Lehigh University IACUC Protocol 66.

Acknowledgements
We thank L. Cassimeris and M. Falk for their intellectual input and assistance with initial phases of the project, and N. Kley and A. Savitzky for early reviews of the manuscript.

Competing interests
The authors declare no competing financial interests.

Author contributions
D.C. and M.C. conceived the project. M.C., S.P. and C.F.-A. designed and executed all experiments. S.P. and C.F.-A. contributed to the TEM work, and S.P., C.F.-A., M.C. and D.C. contributed to the interpretation of findings. M.C. drafted the manuscript, and M.C., S.P., D.C. and C.F.-A. contributed to revisions.

Funding
This study was partially supported by a graduate Grant-In-Aid of Research from the Sigma Xi Scientific Research Society.

Supplementary material
Supplementary material available online at
http://jeb.biologists.org/lookup/suppl/doi:10.1242/jeb.097634/-/DC1

References

Close, M. and Cundall, D. (2014). Snake lower jaw skin: extension and recovery of a hyperextensible keratinized integument. *J. Exp. Zool.* **321**, 78-97.
Dulhunty, A. F. and Franzini-Armstrong, C. (1975). The relative contributions of the folds and caveolae to the surface membrane of frog skeletal muscle fibres at different sarcomere lengths. *J. Physiol.* **250**, 513-539.
Herrel, A., Meyers, J. J., Timmermans, J.-P. and Nishikawa, K. C. (2002). Supercontracting muscle: producing tension over extreme muscle lengths. *J. Exp. Biol.* **205**, 2167-2173.
Linke, W. A., Ivemeyer, M., Mundel, P., Stockmeier, M. R. and Kolmerer, B. (1998). Nature of PEVK-titin elasticity in skeletal muscle. *Proc. Natl. Acad. Sci. USA* **95**, 8052-8057.
Purslow, P. P. (1989). Strain-induced reorientation of an intramuscular connective tissue network: implications for passive muscle elasticity. *J. Biomech.* **22**, 21-31.
Purslow, P. P., Wess, T. J. and Hukins, D. W. L. (1998). Collagen orientation and molecular spacing during creep and stress-relaxation in soft connective tissues. *J. Exp. Biol.* **201**, 135-142.
Salviati, G., Betto, R., Ceoldo, S. and Pierobon-Bormioli, S. (1990). Morphological and functional characterization of the endosarcomeric elastic filament. *Am. J. Physiol.* **259**, C144-C149.
Tskhovrebova, L., Trinick, J., Sleep, J. A. and Simmons, R. M. (1997). Elasticity and unfolding of single molecules of the giant muscle protein titin. *Nature* **387**, 308-312.
Wang, K. and Ramirez-Mitchell, R. (1983). A network of transverse and longitudinal intermediate filaments is associated with sarcomeres of adult vertebrate skeletal muscle. *J. Cell Biol.* **96**, 562-570.
Wang, K., McCarter, R., Wright, J., Beverly, J. and Ramirez-Mitchell, R. (1993). Viscoelasticity of the sarcomere matrix of skeletal muscles. The titin-myosin composite filament is a dual-stage molecular spring. *Biophys. J.* **64**, 1161-1177.

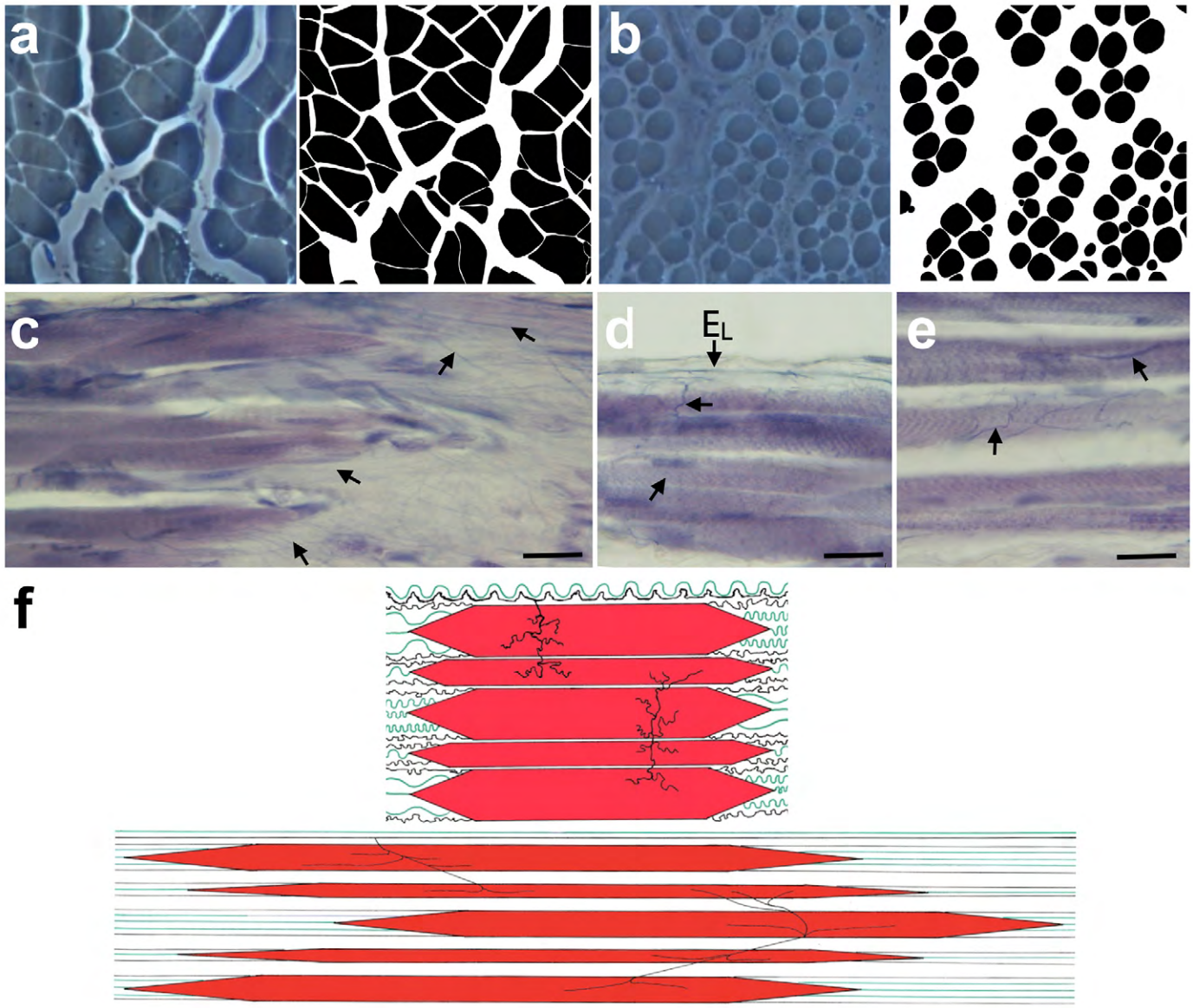

Fig. S1. Histological effects of IMAA extension. (a,b) Light micrographs of cross-sections of resting (a) and stretched (b) muscle stained with Toluidine Blue and accompanying two-tone tracings illustrating the drastic change in muscle fiber shape and cross-sectional area upon extension. (c–e) Light micrographs of moderately stretched muscle stained with iron gallein showing the distribution of elastin fibers (some denoted by arrows) at the insertion on the midline raphe (c), anterior border of the muscle belly (d), and in the middle of the muscle belly (e). At the insertion, the muscle fibers are staggered in this moderately stretched condition, suggesting that fibers are able to move independent of one another depending on the length and extensibility of tendon fibers. Fine elastin filaments radiate from the myotendinous junction into the interramal pad. At the anterior portion of the muscle belly, a lamina of elastin (E_L) can be seen along the convoluted collagenous epimysium, and elastin filaments radiate inward and attach to the peri- and endomysia of adjacent fibers. Thick elastin fibers radiate from endo- and perimysia between adjacent fibers and anchor to similar locations. Scale bars = 8 μm. (f) A two-dimensional model of whole muscle passive stretching. Initially, collagen (green) and elastin (black) are highly convoluted in regions that will ultimately be displaced away from the origin and insertion during an extension event, but are less convoluted in regions that are tightly anchored. At the point beyond which individual fibers are maximally extended (~210% resting length), fibers begin to slip relative to one another as the intramuscular extracellular matrix begins to adjust relative to the plane of extension. At this point, collagen fibrils become taught and elastin becomes highly extended. Recovery from this state of extreme strain (>287% resting length) requires elastic recoil provided by the extended elastin.

Table S1. Summary of anatomical and ultrastructural data for resting, stretched, and recovered snake MIAA muscles.

	Resting	Stretched	Recovered
Total Muscle Length (mm)	2.6±0.061 (n=2)	7.0±0.41 (n=2)	2.7±0.14 (n=2)
Sarcomere Length (μm)	2.63±0.02 (n=189)	5.49±0.87 (n=119)	2.15±0.21 (n=63)
Z-line –A Band (μm)	0.55±0.04 (n=30)	1.92±0.33 (n=30)	0.32±0.07 (n=30)
Gap (μm)	0	0.82±0.15 (n=25)	0
Longitudinal $Z\text{-line}_{fibril1}$ to $Z\text{-line}_{fibril2}$ distance (μm)	0.13±0.11 (n=100)	0.46±0.37 (n=100)	0.09±0.12 (n=100)

All values are mean±s.d. For total muscle length, means represent measurements from both right and left sides of same individual.